Smart Structures and Systems, *Vol. 29, No. 1 (2022) 105-116*
https://doi.org/10.12989/sss.2022.29.1.105

Condition assessment of stay cables through enhanced time series classification using a deep learning approach

Zhiming Zhang*[1], Jin Yan [2], Liangding Li [3], Hong Pan [4] and Chuanzhi Dong [5]

[1] *School for Engineering of Matter, Transport and Energy, Arizona State University, Tempe, AZ, USA*
[2] *Palo Alto Research Center, Palo Alto, CA, USA*
[3] *Department of Computer Science, University of Central Florida, Orlando, FL, USA*
[4] *Department of Civil and Environmental Engineering, North Dakota State University, Fargo, ND, USA*
[5] *Department of Civil, Environmental, and Construction Engineering, University of Central Florida, Orlando, FL, USA*

(*Received April 14, 2021, Revised July 16, 2021, Accepted July 22, 2021*)

Abstract. Stay cables play an essential role in cable-stayed bridges. Severe vibrations and/or harsh environment may result in cable failures. Therefore, an efficient structural health monitoring (SHM) solution for cable damage detection is necessary. This study proposes a data-driven method for immediately detecting cable damage from measured cable forces by recognizing pattern transition from the intact condition when damage occurs. In the proposed method, pattern recognition for cable damage detection is realized by time series classification (TSC) using a deep learning (DL) model, namely, the long short term memory fully convolutional network (LSTM-FCN). First, a TSC classifier is trained and validated using the cable forces (or cable force ratios) collected from intact stay cables, setting the segmented data series as input and the cable (or cable pair) ID as class labels. Subsequently, the classifier is tested using the data collected under possible damaged conditions. Finally, the cable or cable pair corresponding to the least classification accuracy is recommended as the most probable damaged cable or cable pair. A case study using measured cable forces from an in-service cable-stayed bridge shows that the cable with damage can be correctly identified using the proposed DL-TSC method. Compared with existing cable damage detection methods in the literature, the DL-TSC method requires minor data preprocessing and feature engineering and thus enables fast and convenient early detection in real applications.

Keywords: bridge cable; damage detection; deep learning; time series classification

1. Introduction

Stay cables are among the most critical elements of cable-stayed bridges as they provide essential support to the bridge deck Li *et al*. (2018). Stay cables are susceptible to fatigue and corrosion damage which may result in cable deterioration or failure on large span bridges Li and Ou (2016), Brownjohn *et al*. (2011), Ko and Ni (2005). Moreover, when damage occurs to a certain cable, it causes load redistribution among other cables and thus endangers the safety of the whole bridge (Macdonald and Daniell (2005), Miyashita and Nagai (2008). Therefore, the condition assessment of stay cables is of critical importance for ensuring the operation and longevity of cable-stayed bridges Li *et al*. (2014a), Yang *et al*. (2016).

Cable tension monitoring is one of the most widely used approaches for evaluating the health condition of bridge cables Li *et al*. (2014b), with techniques including strain monitoring of cable wires with strain sensors, cable force evaluation with load cell, etc. Li *et al*. (2009, 2014b), Yang *et al*. (2016), Ye *et al*. (2016), Duan *et al*. (2016). A critical challenge faced by this method is that the results of cable tension analysis do not necessarily reflect the health condition of stay cables. This is because the measured cable tension in field tests is not only affected by the cable condition but also many exterior factors, such as traffic loading, environmental influence (wind, temperature, moisture, etc.), and measurement noise Li and Ou (2016). For example, natural frequencies are widely used to evaluate the tension loss of cables Miyashita and Nagai (2008). However, the measured natural frequencies in field tests are largely affected by environmental factors such as temperature. Therefore, it is necessary to develop a health indicator that is sensitive to the cable's damage condition and insusceptible to exterior influences. Li and Ou (2016) used the Gaussian mixture model (GMM) to simulate the measured cable tension ratios between cable pairs and evaluated the cable conditions from the observed transition of model patterns Li and Ou (2016). Despite its performance in cable damage detection, this approach requires intensive data preprocessing, for example clustering corresponding to traffic lanes and source separation, and the used machine learning model is a lot more complex than most deep learning models in the literature. Moreover, the method in Li and Ou (2016) can only identify the cable pair with potential damage and fails to determine the exact damaged cable.

Pattern recognition and machine learning (ML) have been widely used in SHM since the beginning of this

*Corresponding author, Ph.D.,
E-mail: zzhan506@asu.edu

ISSN: 1738-1584 (Print), 1738-1991 (Online)

decade Gui *et al*. (2017), Pan *et al*. (2018), Zhang *et al*. (2019a, 2021), Zhang (2020), Zhang and Sun (2020a, b, c). Applications include data compression and recovery, anomaly detection, knowledge discovery for structural condition assessment, etc. Bao *et al*. (2019a), Sun *et al*. (2020). For example, deep learning (DL) models such as convolutional neural networks (CNN) and recurrent neural networks (RNN) have been widely used for time series analysis in SHM. CNN has been used to analyze measured acceleration series for bolt loosening detection Abdeljaber *et al*. (2018) and structural damage localization Wang and Chan (2009), Lin *et al*. (2017). RNN, including the long short-term memory (LSTM) and gated recurrent unit (GRU), has been used for remaining life estimation Zheng *et al*. (2017) and degradation assessment Guo *et al*. (2017) of machines and response prediction in structural dynamics Zhang *et al*. (2020). It is noted that in SHM, most collected raw data (acceleration, strain, temperature, etc.) are in the form of time series, which need to be further processed and analyzed to evaluate possible structural damage or deficiency. Pattern recognition through DL has the potential of detecting the possible variation/transition of structural health condition using the measured time series data.

Among the ML/DL approaches for time series analysis, time series classification (TSC) has been widely used for data mining and knowledge discovery in various areas, such as health care Abdelfattah *et al*. (2018), Ma *et al*. (2018), Fawaz *et al*. (2018), financial analysis Higdon *et al*. (2019), Luo *et al*. (2019), and weather forecast Gao *et al*. (2019). Given a set of time series data with corresponding class labels, a TSC model is trained to predict the labels of new time series data. TSC methods include feature-based approaches based on non-deep ML models Orsenigo and Vercellis (2010), Seto *et al*. (2015), Xing *et al*. (2010) and DL approaches (i.e., DL-TSC) Fawaz *et al*. (2019), Zheng *et al*. (2014). Compared with feature-based approaches, DL approaches obviate the demanding work of feature extraction and feature engineering. Comprehensive reviews of DL approaches for TSC can be found in Fawaz *et al*. (2019), Santos and Kern (2016), Längkvist *et al*. (2014). Karim *et al*. (2017, 2019a, b) proposed augmenting the fully convolutional networks (FCN) with the long short term memory recurrent neural network (LSTM-RNN) module for TSC. The proposed LSTMFCN model avoids complex data preprocessing and outperforms traditional TSC models in terms of classification accuracy. Experimental studies approve that concatenating the LSTM features with the CNN features improves the robustness of the learned TSC classifier.

Considering the limitations of existing methods for cable condition assessment, this study proposes detecting cable damage through pattern recognition via DL-TSC. The LSTM-FCN model is used in this study for TSC because of its outstanding advantages over other models. The measured cable forces (or their ratio between cable pairs) are taken as the input data of the TSC model and the cable (or cable pair) ID as class labels. A TSC model is first trained and validated using the data measured from intact cables. When damage occurs to a certain cable (or cable pair), its behavior pattern underlying the cable force series should have transitioned to a different state. As a result, the previously learned model from intact conditions will not generalize well when tested on the data measured from a damaged cable (or cable pair), while it still predicts the labels of data from undamaged cables with high accuracy. Therefore, the damaged cable (or cable pair) is expected to be recognized by comparing the testing accuracies. A case study is implemented with field test data measured from a real cable-stayed bridge to validate the proposed methodology. The results show that the correct damaged cable in addition to the damaged cable pair can be correctly identified using the proposed DL-TSC method. Compared with existing methods for cable damage detection, the DL-TSC method obviates the intensive work for data preprocessing or feature engineering without sacrificing the identification accuracy. Therefore, it has advanced convenience and efficiency in practical applications on real bridges. The key contributions of this study include:

(1) Establishing a comprehensive framework for cable damage detection from measured cable forces through pattern recognition via DL-TSC.
(2) Designing the TSC scheme properly so that it successfully captures the pattern transition when damage occurs to certain cables.
(3) Designing two TSC scenarios with different input data and class labels so that their outcomes can be synergistically combined to determine the most probable damaged cable.
(4) Visualizing the time series data in a reduced dimensional space to demonstrate the potential of the proposed DL-TSC method for cable damage detection.
(5) Integrating LSTM features with the CNN features to improve the robustness of TSC with cable force data using the LSTM-FCN model.
(6) Validating the DL-TSC method using field test data from a large-span cable-stayed bridge.

2. Methodology

In this study, the health conditions of stay cables are evaluated through pattern recognition via DL-TSC. Fig. 1 illustrates the framework of the DL-TSC method. This method contains two modules: (1) the module for model training; (2) the module for model testing. The training module starts from data collection under intact conditions. Stay cables can be regarded as intact within the first several months after they are installed or replaced and calibrated. During this period, sufficient data can be collected from the instrumented cables. In this study, cable force data are used to train a TSC model for cable condition assessment. Preprocessing may be necessary to eliminate outliers from malfunctioning sensors. The measured time series data from each cable are divided into n segments (data 1, 2, ..., n in Fig. 1), and each data segment is labeled with its corresponding cable ID (cable I, J, K, etc. in Fig. 1). Hence, a multiclass TSC problem can be formulated with the collection of data segments set as input and the IDs of all instrumented cables as target labels. The number of classes

equals the number of monitored cables. A TSC model is trained and validated using all the labeled data measured under intact conditions. It is expected to have sufficient robustness with respect to the variations of exterior factors by virtue of the merits of DL approaches for pattern recognition and data sufficiency. For convenience, this model is termed model M0.

The testing module evaluates the cable conditions during regular bridge inspection or after disasters like earthquakes or incidents such as vehicle collision. Time series data are collected from instrumented cables and processed in the same format as in the training module. The previously learned model M0 is tested on the new data series. In case a certain cable is still intact without nontrivial damage, its mechanical behavior should lie in the same pattern as its intact condition defined in the training module, and the new measured data should be encompassed by the data collected from the same cable in the training module if visualized in the hyperspace. As a result, the data segments collected therefrom should be correctly labeled using model M0. In contrast, when significant rupture happens to the wires of a certain cable, its mechanical behavior varies. Thus, the pattern underlying measured data therefrom transitions from its intact condition to damaged condition, and the data lies away from their intact counterparts in the hyperspace. Consequently, when the measured data are inputted into model M0, the model cannot output the correct label because the damaged condition has not been incorporated in the model training. In this way, the cable(s) with nontrivial damage can be detected by identifying the one(s) with abnormally low testing accuracy using model M0. It is noted that the classification accuracy for a certain class is evaluated as the average accuracy of all data segments belonging to that class.

Two scenarios with different TSC model inputs are investigated in this study for cable condition assessment: (1) time series of cable forces are taken as input; (2) cable force ratios between cable pairs are taken as input. The nomenclature for Scenario 1 is used in the context above and in Fig. 1 for the convenience of explaining the DL-TSC method. Scenario 2 considers the possible variation of force distribution between cable pairs when damage occurs to a certain cable. When certain cable damages, more portions of forces will be imposed on the other cable in the same cable pair. Li *et al*. (2018) has shown that the cable force ratio within a certain cable pair is an efficient indicator of cable condition. Therefore, this study uses the cable force ratio as the input of the TSC model in Scenario 2. When implementing the DL-TSC method, the difference of Scenario 2 from Scenario 1 is summarized as follows: (1) the input is changed from cable forces to cable force ratios; (2) the class labels are changed from cable IDs to the IDs of cable pairs; (3) the number of total classes is reduced by half. In this study, the recommendations from the two scenarios regarding cable damage conditions will be combined to determine the most probable damaged cable, as the results in these two scenarios are not independent but complementary for the decision making.

The LSTM-FCN model is used for TSC in this study for cable condition assessment, considering its proven advantages over other TSC models Karim *et al*. (2017, 2019a, b). FCN, consisting of temporal convolutions, has been widely used for extracting features from time series data Wang *et al*. (2017). In the LSTM-FCN model, FCN is comprised of temporal convolutional networks that contain several (say L) convolutional layers. The convolutional filter of each layer (e.g., the l^{th} layer) is parameterized by the weight $W^{(l)}$ and the bias $b^{(l)}$ parameters. The ReLU activation function is used, such that in which $f(\cdot)$ is a rectified linear unit.

$$\hat{E}_{i,t}^{(l)} = f\left(b_i^{(l)} + \sum_{t'=1}^{d} < W_{i,t',.}^{(l)}, E_{.,t+d-t'}^{(l-1)} >\right) \tag{1}$$

In the LSTM-FCN model, the FCN is augmented with an LSTM block for improved TSC performance. In the LSTM RNN, the vanishing gradient problem of general

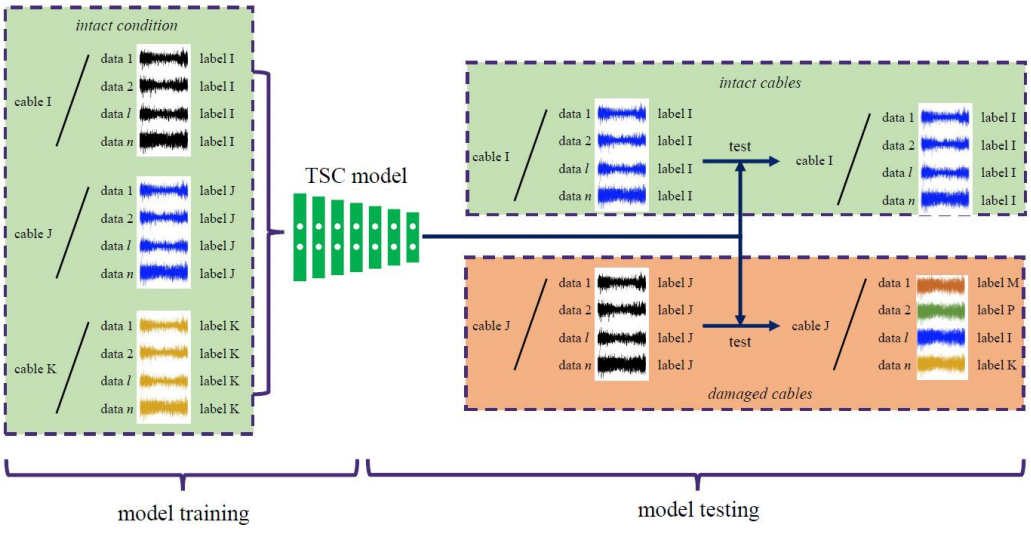

Fig. 1 Framework of the DL-TSC method for condition assessment of stay cables

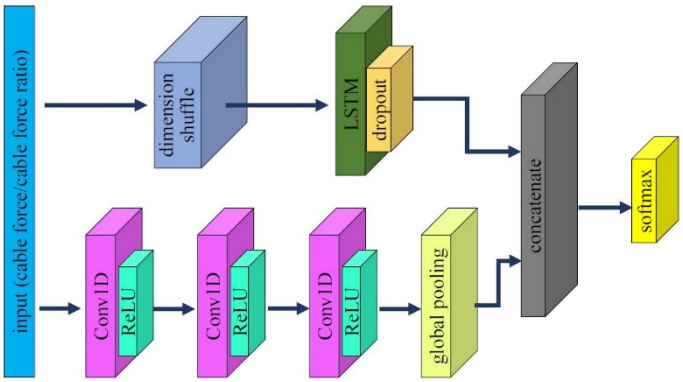

Fig. 2 Architecture of LSTM-FCN (reproduced from Karim *et al*. (2017))

Two scenarios with different TSC model inputs are investigated in this study for cable condition assessment: (1) time series of cable forces are taken as input; (2) cable force ratios between cable pairs are taken as input. The

RNNs has been overcome by introducing gating functions into the network state dynamics. In LSTM, the state updates and outputs are controlled by the hidden vector h and the memory vector m. At time t, the system updates are shown in Eq. (2). Furthermore, the attention mechanism in LSTM enhances its capability of learning long term dependencies existing in long sequences.

$$\begin{aligned} \boldsymbol{g}^u &= \sigma(\boldsymbol{W}^u \boldsymbol{h}_{t-1} + \boldsymbol{I}^u \boldsymbol{x}_t) \\ \boldsymbol{g}^f &= \sigma(\boldsymbol{W}^f \boldsymbol{h}_{t-1} + \boldsymbol{I}^f \boldsymbol{x}_t) \\ \boldsymbol{g}^o &= \sigma(\boldsymbol{W}^o \boldsymbol{h}_{t-1} + \boldsymbol{I}^o \boldsymbol{x}_t) \\ \boldsymbol{g}^c &= \tanh(\boldsymbol{W}^c \boldsymbol{h}_{t-1} + \boldsymbol{I}^c \boldsymbol{x}_t) \\ \boldsymbol{m}_t &= \boldsymbol{g}^f \odot \boldsymbol{m}_{t-1} + \boldsymbol{g}^u \odot \boldsymbol{g}^c \\ \mathbf{h}_t &= \tanh(\boldsymbol{g}^o \odot \boldsymbol{m}_t) \end{aligned} \tag{2}$$

in which σ is the logistic sigmoid function; $\odot$ represents element-wise multiplication; W^u, W^f, W^0, and W^c are recurrent weight matrices; I^u, I^f, I^0, and I^c are projection matrices.

Fig. 2 illustrates the architecture of the LSTM-FCN model that is used in this study for univariate TSC. It consists of an FCN module and an LSTM module. The FCN module contains three stacked temporal convolutional blocks, and the kernel sizes will be determined later in the EXPERIMENTAL STUDY section. Each temporal convolutional block consists of a temporal convolutional layer for feature extraction and a ReLU activation function. At the end of the FCN module, global average pooling is imposed on the output of the final convolutional block to reduce the number of parameters in the FCN model and thus decrease its complexity.

In the LSTM-FCN model, the LSTM module is used to augment the feature vector obtained from FCN. It acts as a regularizer to FCN and thus is expected to improve its robustness. The LSTM module is comprised of a dimension shuffle block and a regular LSTM block consisting of an LSTM layer with dropout. It is worth noting that in the LSTM-FCN model, the FCN module and the LSTM module process the input time series differently. The FCN module takes the input as a univariate time series having many time steps. In contrast, in the LSTM module, dimension shuffle is implemented first to transform the multi-step time series into a multivariate time series with a single time step. It has been proved that dimension shuffle can reduce the rapid overfitting issue of the LSTM model and thus improve the accuracy and efficiency of the LSTM-FCN model in TSC Karim *et al*. (2017, 2019a, b). Finally, the features extracted from the FCN and LSTM modules are concatenated and passed to a softmax layer for multiclass labeling. The LSTM-FCN model has been used in radar image processing Teimouri *et al*. (2019), video processing Xu *et al*. (2017), aero-engine prognosis Zhang *et al*. (2019b), etc.

3. Experimental study

In this section, an experimental study is implemented to validate the proposed DLTSC method for condition assessment of stay cables using the data measured from a large-span cable-stayed bridge in Mainland China Li *et al*. (2018). The cable force data and related resources are provided by the organizing committee of the 1st

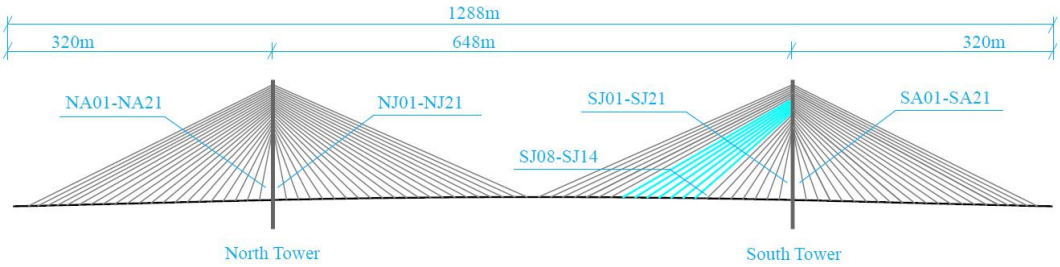

Fig. 3 The cable-stayed bridge used for the experimental study Li *et al*. (2018)

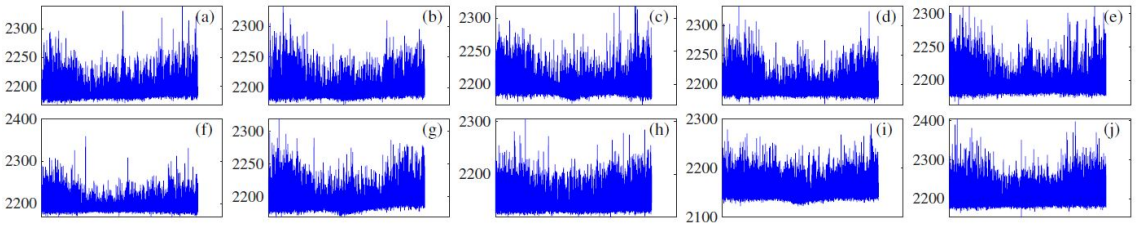

Fig. 4 Cable force of SJS08 with the unit kN. (a) to (j) show the data on the following 10 days respectively: 2006-05-13 to 2006-05-19, 2007-12-14, 2009-05-05, and 2011-11-01

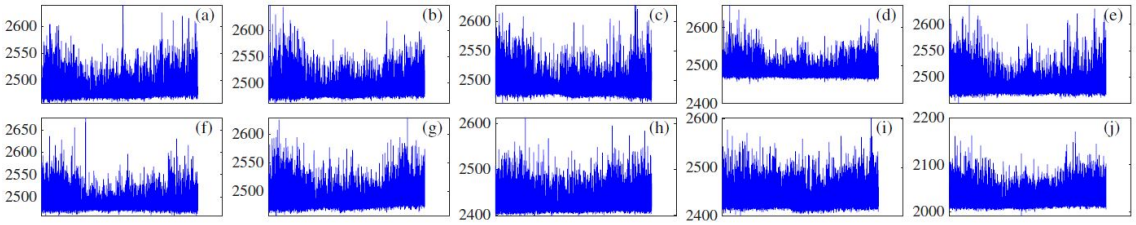

Fig. 5 Cable force of SJS11 with the unit kN. (a) to (j) show the data on the following 10 days respectively: 2006-05-13 to 2006-05-19, 2007-12-14, 2009-05-05, and 2011-11-01

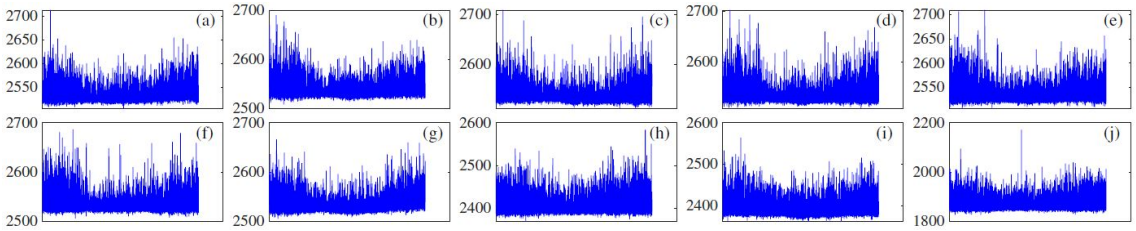

Fig. 6 Cable force of SJX11 with the unit kN. (a) to (j) show the data on the following 10 days respectively: 2006-05-13 to 2006-05-19, 2007-12-14, 2009-05-05, and 2011-11-01

International Project Competition for Structural Health Monitoring (IPC-SHM 2020). More details about the bridge and data can be found in Li *et al*. (2018), Tang *et al*. (2019), Bao *et al*. (2019a, b), Xu *et al*. (2019), Spencer *et al*. (2019), Bao and Li (2020). This bridge has a main span of 648 m and two side spans of 320 m as shown in Fig. 3. The bridge deck is supported by a total of 168 stay cables (i.e., 64 pairs), which are labeled according to their locations as shown in Fig. 3. Letters "N" and "S" in the figure denote the north tower and south tower side, respectively; letters "A" and "J" denote the bank side and river side, respectively; letters "S" and "X" denote the upstream and downstream side, respectively. For example, SJ11 denotes the 11th cable pair on the south tower side, and it contains cable SJS11 on the upstream side and cable SJX11 on the downstream side.

All 168 cables were installed with anchorage load cells having a sampling frequency of 2 Hz. The cables have been monitored with the installed sensors since October in 2005. In this study, 14 cables (i.e., 7 cable pairs from SJ08 to SJ14) among the 168 cables are investigated for stay cable condition assessment, with all the rest of the cables assumed intact. Cable forces measured on 10 days (i.e., 2006-05-13 to 2006-05-19, 2007-12-14, 2009-05-05, and 201111-01) are available for analysis and decision making regarding the cable damage condition. All the 14 investigated cables remained intact before 2011, and wire rupture occurred to a certain cable in 2011 (prior to the day 2011-11-01). This case aims to identify the damaged cable among these 14 cables using the measured cable forces.

In the rest of this section, the measured cable forces are first preprocessed to eliminate possible outliers and format the time series data to data segments for each class in the two scenarios defined in the METHODOLOGY section. After they are preprocessed, the measured data are visualized in a hyperspace via manifold learning to have a brief view of the data belonging to different classes. Subsequently, An LSTM-FCN model is configured and trained and validated using data collected from all investigated cables under intact conditions, that is, the cable forces measured from the 14 cables on the first 9 days (i.e., 2006-05-13 to 2006-05-19, 2007-12-14, and 2009-05-05). Finally, the learned LSTM-FCN model is tested on the data collected on 2011-11-01. The testing results in the two scenarios are discussed and integrated for decision making regarding the most probable damaged cable.

3.1 Data preprocessing

In Scenario 1, the cable forces are taken as the input of the TSC model. Figs. 4 to 6 show the measured cable forces from three example cables (i.e., SJS08, SJS11, and SJX11).

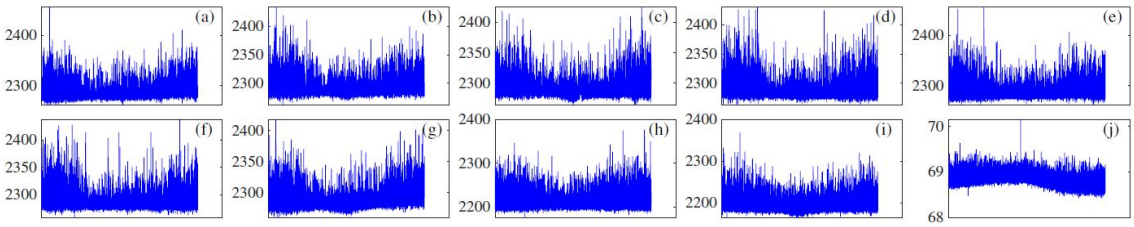

Fig. 7 Cable force of SJX08 with the unit kN. (a) to (j) show the data on the following 10 days respectively: 2006-05-13 to 2006-05-19, 2007-12-14, 2009-05-05, and 2011-11-01

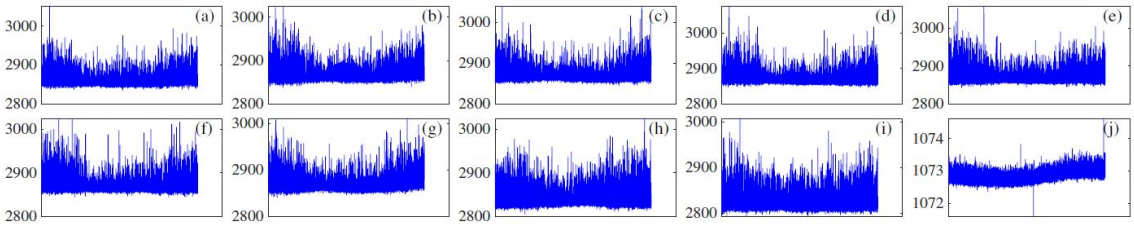

Fig. 8 Cable force of SJX13 with the unit kN. (a) to (j) show the data on the following 10 days respectively: 2006-05-13 to 2006-05-19, 2007-12-14, 2009-05-05, and 2011-11-01

It can be observed that, all cable forces show a strong daily periodicity pattern, most probably due to changes in traffic loads or environmental conditions such as temperature variations. In data preprocessing, extreme values exceeding the thresholds of cable forces are excluded from the data record.

Fig. 7 shows the cable forces measured on SJX08. It can be observed that on the day 2011-11-01 (Fig. 7(j)), the measured cable force is notably small compared with that on prior dates. Additionally, the amplitude fluctuation is within 2 kN on that day, which is much smaller than that of previous dates (i.e., approximately 100 kN). This abnormal pattern indicates possible cable damage or sensor failure.

Moreover, the cable force exhibits a reversal or random drift pattern that does not change with the traffic loads or environmental conditions. Therefore, it can be determined that the load cell on SJX08 failed prior to 201111-01. A similar phenomenon is observed on the cable SJX13, as shown in Fig. 8(j). Sensor failure causes apparent pattern change of measured signals, which, however, does not indicate the pattern transition of cable behaviors due to damage occurrence. Thus, it is difficult to determine whether these two cables are still intact or damaged on the last day using the measured signals. Therefore, cables SJX08 and SJX13 are excluded for damage detection in the rest of this paper. Nevertheless, the data measured on these

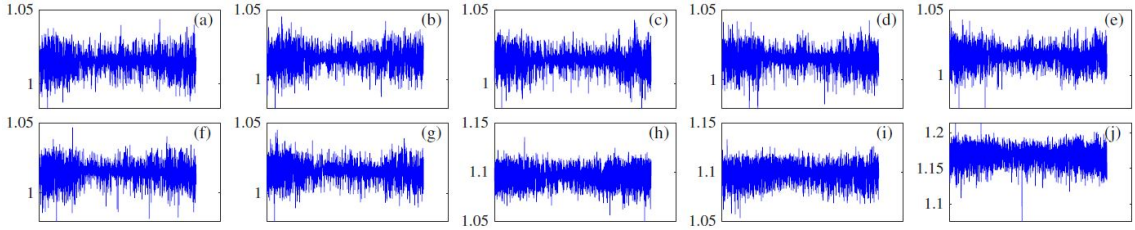

Fig. 9 Cable force ratio of SJ09. (a) to (j) show the data on the following 10 days respectively: 2006-05-13 to 2006-05-19, 2007-12-14, 2009-05-05, and 2011-11-01

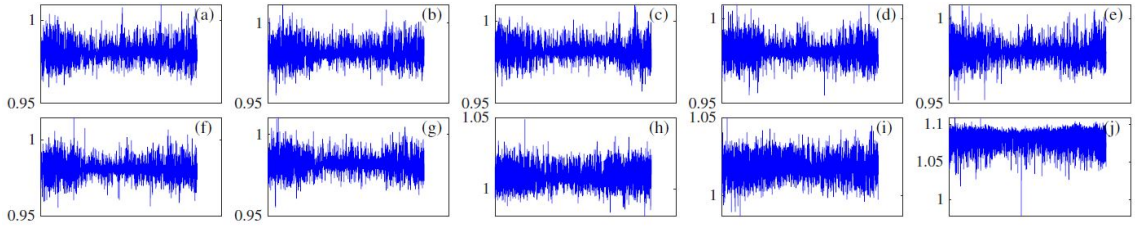

Fig. 10 Cable force ratio of SJ11. (a) to (j) show the data on the following 10 days respectively: 2006-05-13 to 2006-05-19, 2007-12-14, 2009-05-05, and 2011-11-01

two cables under intact conditions are still used in training and validating a TSC model in both scenarios.

In Scenario 2, the cable force ratios between cable pairs are taken as the input of the TSC model. In this case study, the cable force ratio of a cable pair (e.g., SJ08) is defined as the cable force of the upstream cable (e.g., SJS08) divided by that of the downstream cable (e.g., SJX08). Figs. 9 and 10 show the cable force ratios of two example cable pairs, SJ9 and SJ11, respectively. It can be observed that all the cable force ratios fluctuate around a certain value close to 1.0, most probably because the force distribution between the two cables in a pair is approximately equal when a vehicle crosses this cable pair regardless of which lane it travels in. Moreover, Fig. 10 shows that the times series of cable force ratio of SJS11 appears fluctuating in a different mode on 2011-11-01 (Fig. 10(j)) than on prior dates (Figs. 10(a) to (i)). This phenomenon is not observed in the cable forces of each cable in this pair as shown in Figs. 5 and 6. Hence, it can be conjectured that the cable force ratio may contain additional information regarding the variation of cable conditions, which though needs further examination via pattern recognition.

For a certain cable, the cable force series measured on each day has a length of 172800, so does the cable force ratio for a certain cable pair. In this case study, each time series of cable force or cable force ratio is divided into 108 segments, each having a length of 1600. This data segmentation follows the practice of the UCR datasets Dau *et al*. (2019) that are widely used for TSC. Each data segment is labeled with the cable or cable pair ID it belongs to. Hence, each class contains 108 × 9 = 972 times series samples in the training dataset (9 days prior to 2011) and 108 samples in the testing dataset (1 day in 2011). It is noted that the TSC problem has 14 class labels when taking the cable forces as input (Scenario 1) and 7 class labels when taking the cable force ratios as input (Scenario 2). Fig. 11 shows the process of data segmentation and labeling ((a) to (c)) and the prepared data in Scenario 1(d). No further preprocessing is implemented, as the LSTM-FCN model requires minimal preprocessing for TSC Karim *et al*. (2017, 2019a, b). With the data prepared for multiclass TSC, they are first visualized in the hyperspace via manifold learning in the next section (Data Visualization) before being fed into a TSC model.

3.2 Data visualization

In this section, the time series data (cable force and cable force ratio) are visualized in a 2D space to provide a brief view of the distribution of data belonging to difference classes in the hyperspace and the potential effects of damage occurrence on the distribution. The manifold learning is conducted via uniform manifold approximation and Projection (UMAP) McInnes *et al*. (2018) to reduce the dimension of temporal features in the time series data, such that they can be represented in a low dimensional embedding. UAMP is a dimension reduction technique that has been widely used for data visualization. This manifold learning technique combines the Riemannian geometry and the algebraic topology for dimension reduction. In UMAP, the topological representation of high-dimension data series is established using the patches, local manifold approximation, and the representations of local fuzzy simplicial set. The layout of data representation is then optimized in the low dimensions with the criterion set as the cross-entropy between topological representations.

The cost function of UMAP is the cross-entropy of two fuzzy sets which is represented by symmetric weight matrices. That is in which v_{ij} are symmetrized input affinities. The output weights are given by

$$C_{UMAP} = \sum_{ij}\left[v_{ij}\log\left(\frac{v_{ij}}{w_{ij}}\right) + (1-v_{ij})\log\left(\frac{1-v_{ij}}{1-w_{ij}}\right)\right] \quad (3)$$

in which v_{ij} are symmetrized input affinities. The output weights are given by

$$w_{ij} = 1/\left(1 + ad_{ij}^{2b}\right) \quad (4)$$

in which a and b are determined by non-linear least squares fit. The additional term in the cost function enables the UMAP to capture the global data structure compared with tSNE which simply simulates the local structure at moderate perplexity values. The unsymmetrized UMAP input weights are computed as

$$v_{j|i=\exp[-(r_{ij}-\rho_i)/\sigma_i]} \quad (5)$$

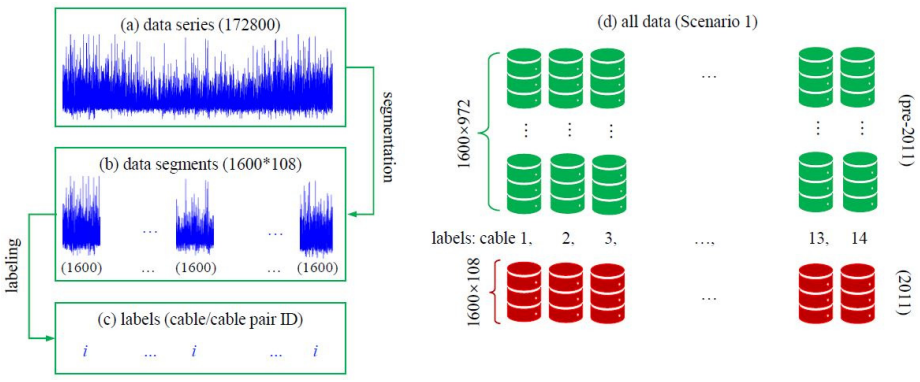

Fig. 11 Data segmentation and labeling in preprocessing

(a) (b)

Fig. 12 Low dimensional representation of (a) cable force; and (b) cable force ratio. pre-2011: data collected before 2011

in which r_{ij} are the input distances, ρ_i is the distance to the nearest neighbor, and σ_i is analogous to β_i in the perplexity calibration in SNE.

Compared with other manifold learning methods such as t-SNE, UMAP has superior advantages in global structure preservation, computational efficiency, and generality in dimension reduction. It is worth noting that manifold learning has been used for structural damage detection in Xu and Liu (2021). More details about the manifold learning method can be found in McInnes *et al*. (2018), Xu and Liu (2021), Cayton (2005), Talwalkar *et al*. (2008).

Fig. 12(a) shows the low dimensional representation of cable force data collected from two example cables, i.e., SJS11 and SJX14. It can be observed that the cable force data collected from SJS11 and SJX14 before 2011 and SJX14 in 2011 are well clustered with considerable variation due to the change of exterior excitations. In contrast, the data from SJS11 in 2011 are clustered in a different pattern with all the data gathering in a very small region. Similar phenomenon can be observed in the low dimensional representation of cable force ratio in Fig. 12(b). The data measured from cable pair SJ11 in 2011 has a very different clustering pattern from other datasets. This significant difference in clustering pattern may indicate possible state transition on cable SJS11 and cable pair SJ11 in 2011, which will be further investigated in the rest of this paper via TSC.

3.3 LSTM-FCN model configuration

As shown in Fig. 2, the LSTM-FCN model contains two modules for feature extrac¬tion, namely, the FCN module and the LSTM module. The FCN module has three 1D convolutional layers in the temporal convolutional blocks. For this case study, the kernel sizes are set as 128, 256, and 128, respectively, for the three convolutional layers after trial analysis. Regarding the LSTM module, the optimal number of LSTM cells is determined as 8 through a hyperparameter search over a range of 4 cells to 128 cells. The dropout rate is set as high as 80% to avoid overfitting.

The number of training epochs is set as 2000, and the initial batch size is set as 128. All models in this study are trained using the Keras library with the TensorFlow backend. The Adam optimizer is used in the model training with an initial learning rate of 0.001 and a final learning rate of 0.0001, which is reduced by $\frac{1}{\sqrt[3]{2}}$ every 100 epochs if no improvement of the validation performance is observed. The strategy proposed in He *et al*. (2015) is used to initialize all convolutional kernels. The classification accuracy is used as the criterion for evaluating the results of model testing.

4. Results and discussions

As indicated in Fig. 1 for the framework of the DL-TSC method, an LSTM-FCN TSC model is first trained and validated using the intact data collected on the first 9 days (i.e., 2006-05-13 to 2006-05-19, 2007-12-14, 2009-05-05). Subsequently, the learned model is tested on the data collected on 2011-11-01 for decision making regarding the cable damage conditions. This section first presents and discusses the results of model testing for the two investigated scenarios, including the classification accuracy on the validation dataset prior to 2011, the classification accuracy on all data in 2011, and the classification accuracy on the data for each cable or cable pair in 2011. Finally, the most probable damaged cable is recommended by combining the testing results in the two scenarios.

4.1 Scenario 1 with cable force as input

Table 1 compares the testing accuracies of all datasets in Scenario 1. Columns 2 and 3 list the overall testing accuracy on the data collected on the first 9 days prior to 2011 (i.e., 2006-05-13 to 2006-05-19, 2007-12-14, 2009-05-05) and the last day in 2011 (i.e., 2011-11-01), respectively. Columns 4 to 10 list the testing accuracy on the data collected from each cable on 2011-11-01. The overall testing accuracy on the intact data (pre-2011) is 0.79, which is not as high as expected, most probably because the cable force magnitude itself is not directly related to the cable properties or damage conditions. When tested on the unseen data in 2011, the model yields an overall accuracy of as low as 0.56. This considerable reduction of classification accuracy indicates that the learned TSC model using the intact data fails to generalize well on the data collected on 2011-11-01. This lack of generalization reflects possible variation of cables' behavior pattern and thus potential damage occurrence on a certain cable. In detail, the testing accuracies on SJS11 and SJX10 are both around 0.25 and considerably lower than that on other cables which are all above 0.50. The classification accuracy on the two cables with malfunctioning sensors

Table 1 Testing accuracies on different datasets in Scenario 1

Dataset	Pre-2011	Overall-2011	SJS08	SJS09	SJS10	SJS11	SJS12	SJS13	SJS14
Accuracy	0.79	0.56	0.53	0.69	0.59	0.28	0.65	0.89	0.55
Dataset	-	-	SJX08	SJX09	SJX10	SJX11	SJX12	SJX13	SJX14
Accuracy	-	-	-	0.83	0.25	0.60	0.61	-	0.60

*Pre-2011: data collected before 2011; Overall-2011: all data in 2011

Table 2 Testing accuracies on different datasets in Scenario 2

Dataset	Pre-2011	Overall-2011	SJS08	SJS09	SJS10	SJS11	SJS12	SJS13	SJS14
Accuracy	0.96	0.75	-	0.94	0.95	0.02	.94	-	0.91

*Pre-2011: data collected before 2011; Overall-2011: all data in 2011

(i.e., SJX08 and SJX13) is not applicable.

From this comparison of classification accuracy between cables, one can hypothesize that damage may have occurred to one or both of cables SJS11 and SJX10 before 2011-11-01. These two cables are located very close to each other, as shown in Fig. 3. Hence, it is challenging to determine whether one of them has been damaged or both of them since damage on a certain cable can significantly affect the behavior of adjacent cables. It is even more difficult to determine which one of these two cables is more probably damaged, especially considering that their testing accuracies are very close. Considering the insufficient overall classification accuracy (i.e., 0.79 for pre-2011 data and 0.56 for overall-2011), further investigation is necessary before the final decision can be made.

4.2 Scenario 2 with cable force ratio as input

The testing results on all datasets in Scenario 2 are compared in Table 2. The overall accuracy on data collected prior to 2011 is 0.96, which is much higher than that in Scenario 1 (i.e., 0.79). This significant increase in testing accuracy approves that the cable force ratio is an enhanced representation of the cable properties and conditions compared with the cable force. Additionally, the overall testing accuracy on data collected in 2011 is also increased from 0.56 to 0.75, which indicates that the learned model from intact data has improved generality on new data. Still, the reduced testing accuracy from 0.96 for pre-2011 data to 0.75 for overall-2011 data indicates possible change of cables' behavior pattern.

Inspecting the testing results on each cable pair, one can find that the accuracies are all above 0.90 except that on SJ11 (i.e., 0.02). This large difference in classification accuracy leads to a confident recommendation that damage should have occurred to one or both cables in the cable pair SJ11. Additionally, the high testing accuracies (above 0.90) on intact cable pairs (all except SJ11) further verify the improved generality of the trained model using intact data compared with that in Scenario 1. The cable pairs with malfunctioning sensors are excluded from this evaluation. Subsequently, the final decision regarding the most probable damaged cable will be made via combining the findings in both scenarios.

4.3 Decision making on the most probable damaged cable

Considering that the findings in Scenario 1 and Scenario 2 are not independent but complementary for decision making, this study combines the results from these two scenarios synergistically to determine the most probable damaged cable. Fig. 13 compares the testing accuracies of each cable or cable pair in the two scenarios. The data

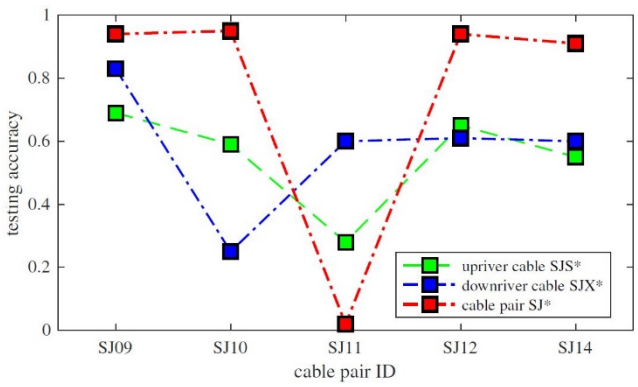

Fig. 13 Comparison of testing accuracies in Scenario 1 and Scenario 2. The testing results on data collected on 2011-11-01 is used in this plot. The curves with legends "upriver" and "downriver" are plotted using the results of Scenario 1, and the curve with "cable pair" is plotted using the results of Scenario 2

collected on 2011-11-01 is used for this comparison, and the cables or cable pairs with malfunctioning sensors are excluded. Testing results in Scenario 1 indicate possible damage among cable SJS11 and SJX10 based on their respective low testing accuracy. Results in Scenario 2 recommend potential damage among the two cables (SJS11 and SJX11) in the cable pair SJ11, which has more confidence level due to the improved model generality and larger difference in testing accuracy. Therefore, combining the results in these two scenarios, the most probable damaged cable can be determined as SJS11. This conclusion has been verified by the organizing committee of the IPC-SHM 2020, and it is consistent with the results in Li *et al*. (2018), which detected damage on the same cable pair but failed to identify the exact damaged cable.

5. Conclusions

Stay cables are the most critical component on a cable-stayed bridge. They are susceptible to fatigue and corrosion damage that may lead to the failure of cables and even the whole bridge. Therefore, early detection of cable damage has critical importance for bridge safety. To this end, this study proposes detecting cable damage from collected cable force data through time series classification (TSC) using the deep learning (DL) framework. The LSTM-FCN model is used in this DL-TSC method because of its merits over other TSC models. A TSC classifier is first trained and validated using the data (cable force in Scenario 1 and cable force ratio in Scenario 2) collected under intact conditions. When tested on the new data with possible damage, the learned classifier yields the least classification accuracy on the time series data collected from the most probable damaged cable or cable pair. Combining the results of the two scenarios, the most probable damaged cable can be identified. An experimental case study using measured data from a large-span cable-stayed bridge is implemented to validate the proposed methodology. Results have proved that the correct damaged cable can be successfully identified using the proposed DL-TSC method. Compared with the methods in the literature, the DL-TSC method requires the least work of data preprocessing and feature engineering, which enables fast and convenient early detection and warning in real applications. It is worth noting that the DL-TSC method has the potential of detecting damage on other types of structures, which will be investigated in future studies.

Acknowledgments

Our team was awarded the 1st prize in the 1st International Project Competition for Structural Health Monitoring (IPC-SHM 2020) for the work presented in this paper. The authors appreciate the essential support from the organizing committee of IPC-SHM 2020 during this competition. More information about this competition can be found in Bao *et al*. (2021), IPC. Additionally, the authors would like to acknowledge the assistance from Mr. Nan Xu, a graduate research assistant at Arizona State University, in visualizing the time series data using the manifold learning method.

References

Abdelfattah, S.M., Abdelrahman, G.M. and Wang, M. (2018), "Augmenting the size of eeg datasets using generative adversarial networks", *Proceedings of 2018 International Joint Conference on Neural Networks* (*IJCNN*), Rio de Janeiro, Brazil, July, pp. 1-6. https://doi.org/10.1109/IJCNN.2018.8489727

Abdeljaber, O., Avci, O., Kiranyaz, M.S., Boashash, B., Sodano, H. and Inman, D.J. (2018), "1-D CNNs for structural damage detection: Verification on a structural health monitoring benchmark data", *Neurocomputing*, **275**, 1308-1317. https://doi.org/10.1016/j.neucom.2017.09.069

Bao, Y. and Li, H. (2020), "Machine learning paradigm for structural health monitoring", *Struct. Health Monitor.*, **20**(4), 1353-1372. https://doi.org/10.1177/1475921720972416

Bao, Y., Chen, Z., Wei, S., Xu, Y., Tang, Z. and Li, H. (2019a), "The state of the art of data science and engineering in structural health monitoring", *Engineering*, **5**(2), 234-242. https://doi.org/10.1016/j.eng.2018.11.027

Bao, Y., Tang, Z., Li, H. and Zhang, Y. (2019b), "Computer vision and deep learning–based data anomaly detection method for structural health monitoring", *Struct. Health Monitor.*, **18**(2), 401-421. https://doi.org/10.1177/1475921718757405

Bao, Y., Li, J., Nagayama, T., Xu, Y., Spencer Jr, B.F. and Li, H. (2021), "The 1st International Project Competition for Structural Health Monitoring (IPC-SHM, 2020): A summary and benchmark problem", *Struct. Health Monitor.*, **20**(4), 2229-2239. https://doi.org/10.1177/14759217211006485

Brownjohn, J.M., De Stefano, A., Xu, Y.L., Wenzel, H. and Aktan, A.E. (2011), "Vibration-based monitoring of civil infrastructure: challenges and successes", *J. Civil Struct. Health Monitor.*, **1**(3-4), 79-95. https://doi.org/10.1007/s13349-011-0009-5

Cayton, L. (2005), "Algorithms for manifold learning", Univ. of California at San Diego Tech. Rep, **12**(1-17), p. 1.

Dau, H.A., Bagnall, A., Kamgar, K., Yeh, C.C.M., Zhu, Y., Gharghabi, S., Ratanamahatana, C.A. and Keogh, E. (2019), "The UCR time series archive", *IEEE/CAA J. Automatica Sinica*, **6**(6), 1293-1305. https://doi.org/10.1109/JAS.2019.1911747

Duan, Y.F., Zhang, R., Dong, C.Z., Luo, Y.Z., Or, S.W., Zhao, Y. and Fan, K.Q. (2016), "Development of Elasto-Magneto-Electric (EME) sensor for in-service cable force monitoring", *Int. J. Struct. Stabil. Dyn.*, **16**(04), 1640016. https://doi.org/10.1142/S0219455416400162

Fawaz, H.I., Forestier, G., Weber, J., Idoumghar, L. and Muller, P.A. (2018), "Evaluating surgical skills from kinematic data using convolutional neural networks", *Proceedings of International Conference on Medical Image Computing and Computer-Assisted Intervention*, pp. 214-21. https://doi.org/10.1007/978-3-030-00937-3_25

Fawaz, H.I., Forestier, G., Weber, J., Idoumghar, L. and Muller, P.A. (2019), "Deep learning for time series classifcation: a review", *Data Min. Knowl. Discov.*, **33**(4), 917-963. https://doi.org/10.1007/s10618-019-00619-1

Gao, M., Li, J., Hong, F. and Long, D. (2019), "Day-ahead power forecasting in a large-scale photovoltaic plant based on weather classification using LSTM", *Energy*, **187**, 115838. https://doi.org/10.1016/j.energy.2019.07.168

Gui, G., Pan, H., Lin, Z., Li, Y. and Yuan, Z. (2017), "Data-driven support vector machine with optimization techniques for structural health monitoring and damage detection", *KSCE J. Civil Eng.*, **21**(2), 523-534.

https://doi.org/10.1007/s12205-017-1518-5
Guo, L., Li, N., Jia, F., Lei, Y. and Lin, J. (2017), "A recurrent neural network based health indicator for remaining useful life prediction of bearings", *Neurocomputing*, **240**, 98-109. https://doi.org/10.1016/j.neucom.2017.02.045
He, K., Zhang, X., Ren, S. and Sun, J. (2015), "Delving deep into rectifiers: Surpassing human-level performance on imagenet classification", *Proceedings of the IEEE International Conference on Computer Vision*, pp. 1026-1034.
Higdon, B.P., El Mokhtari, K. and Başar, A. (2019), "Time-series-based classification of financial forecasting discrepancies", *Proceedings of International Conference on Innovative Techniques and Applications of Artificial Intelligence*, pp. 474-479. https://doi.org/10.1007/978-3-030-34885-4_39
IPC-SHM (2020), http://www.schm.org.cn/#/IPC-SHM,2020
Karim, F., Majumdar, S., Darabi, H. and Chen, S. (2017), "LSTM fully convolutional networks for time series classification", *IEEE Access*, **6**, 1662-1669. https://doi.org/10.1109/ACCESS.2017.2779939
Karim, F., Majumdar, S. and Darabi, H. (2019a), "Insights into LSTM fully convolutional networks for time series classification", *IEEE Access*, **7**, 67718-67725. https://doi.org/10.1109/ACCESS.2019.2916828
Karim, F., Majumdar, S., Darabi, H. and Harford, S. (2019b), "Multivariate LSTM-FCNs for time series classification", *Neural Networks*, **116**, 237-245. https://doi.org/10.1016/j.neunet.2019.04.014
Ko, J.M. and Ni, Y.Q. (2005), "Technology developments in structural health monitoring of large-scale bridges", *Eng. Struct.*, **27**(12), 1715-1725. https://doi.org/10.1016/j.engstruct.2005.02.021
Längkvist, M., Karlsson, L. and Loutfi, A. (2014), "A review of unsupervised feature learning and deep learning for time-series modeling", *Pattern Recogn. Lett.*, **42**, 11-24. https://doi.org/10.1016/j.patrec.2014.01.008
Li, H. and Ou, J. (2016), "The state of the art in structural health monitoring of cable-stayed bridges", *J. Civil Struct. Health Monitor.*, **6**(1), 43-67. https://doi.org/10.1007/s13349-015-0115-x
Li, H., Ou, J. and Zhou, Z. (2009), "Applications of optical fibre bragg gratings sensing technology-based smart stay cables", *Optics Lasers Eng.*, **47**(10), 1077-1084. https://doi.org/10.1016/j.optlaseng.2009.04.016
Li, S., Huang, W., Wang, Z. and Lei, J. (2014a), "Design and aerodynamic investigation of a parallel vehicle on a wide-speed range", *Sci. China Inform. Sci.*, **57**(12), 1-10. https://doi.org/10.1007/s11432-014-5225-2
Li, H., Zhang, F. and Jin, Y. (2014b), "Real-time identification of time-varying tension in stay cables by monitoring cable transversal acceleration", *Struct. Control Health Monitor.*, **21**(7), 1100-1117. https://doi.org/10.1002/stc.1634
Li, S., Wei, S., Bao, Y. and Li, H. (2018), "Condition assessment of cables by pattern recognition of vehicle-induced cable tension ratio", *Eng. Struct.*, **155**, 1-15. https://doi.org/10.1016/j.engstruct.2017.09.063
Lin, Y.Z., Nie, Z.H. and Ma, H.W. (2017), "Structural damage detection with automatic feature-extraction through deep learning", *Comput.-Aided Civil Infrastr. Eng.*, **32**(12), 1025-1046. https://doi.org/10.1111/mice.12313
Luo, C., Jiang, Z. and Zhang, Y. (2019), "A novel reconstructed training-set svm with roulette cooperative coevolution for financial time series classification", *Expert Syst. Applicat.*, **123**, 283-298. https://doi.org/10.1016/j.eswa.2019.01.022
Ma, T., Xiao, C. and Wang, F. (2018), "Health-atm: A deep architecture for multifaceted patient health record representation and risk prediction", *Proceedings of the 2018 SIAM International Conference on Data Mining*, San Diego, CA, USA, pp. 261-269. https://doi.org/10.1137/1.9781611975321.30
Macdonald, J.H. and Daniell, W.E. (2005), "Variation of modal parameters of a cable-stayed bridge identified from ambient vibration measurements and FE modelling", *Eng. Struct.*, **27**(13), 1916-1930. https://doi.org/10.1016/j.engstruct.2005.06.007
McInnes, L., Healy, J. and Melville, J. (2018), "UMAP: Uniform manifold approximation and projection for dimension reduction", arXiv preprint arXiv:1802.03426.
Miyashita, T. and Nagai, M. (2008), "Vibration-based structural health monitoring for bridges using laser doppler vibrometers and mems-based technologies", *Int. J. Steel Struct.*, **8**(4), 325-331.
Orsenigo, C. and Vercellis, C. (2010), "Combining discrete svm and fixed cardinality warping distances for multivariate time series classification", *Pattern Recog.*, **43**(11), 3787-3794. https://doi.org/10.1016/j.patcog.2010.06.005
Pan, H., Azimi, M., Yan, F. and Lin, Z. (2018), "Time-frequency-based data-driven structural diagnosis and damage detection for cable-stayed bridges", *J. Bridge Eng.*, **23**(6), 04018033. https://doi.org/10.1061/(ASCE)BE.1943-5592.0001199
Santos, T. and Kern, R. (2016), "A literature survey of early time series classification and deep learning", In: *SamI40 workshop at i-KNOW'16*, Graz, Austria, October.
Seto, S., Zhang, W. and Zhou, Y. (2015), "Multivariate time series classification using dynamic time warping template selection for human activity recognition", *Proceedings of 2015 IEEE Symposium Series on Computational Intelligence*, Cape Town, South Africa, December, pp. 1399-1406. https://doi.org/10.1109/SSCI.2015.199
Spencer Jr, B.F., Hoskere, V. and Narazaki, Y. (2019), "Advances in computer vision-based civil infrastructure inspection and monitoring", *Engineering*, **5**(2), 199-222. https://doi.org/10.1016/j.eng.2018.11.030
Sun, L., Shang, Z., Xia, Y., Bhowmick, S. and Nagarajaiah, S. (2020), "Review of bridge structural health monitoring aided by big data and artificial intelligence: From condition assessment to damage detection", *J. Struct. Eng.*, **146**(5), 04020073. https://doi.org/10.1061/(ASCE)ST.1943-541X.0002535
Talwalkar, A., Kumar, S. and Rowley, H. (2008), "Large-scale manifold learning", *Proceedings of 2008 IEEE Conference on Computer Vision and Pattern Recognition*, Anchorage, AK, USA, June, pp. 1-8. https://doi.org/10.1109/CVPR.2008.4587670
Tang, Z., Chen, Z., Bao, Y. and Li, H. (2019), "Convolutional neural network-based data anomaly detection method using multiple information for structural health monitoring", *Struct. Control Health Monitor.*, **26**(1), e2296. https://doi.org/10.1002/stc.2296
Teimouri, N., Dyrmann, M. and Jørgensen, R.N. (2019), "A novel spatio-temporal fcn-lstm network for recognizing various crop types using multi-temporal radar images", *Remote Sensing*, **11**(8), 990. https://doi.org/10.3390/rs11080990
Wang, F. and Chan, T. (2009), "Review of vibration-based damage detection and condition assessment of bridge structures using structural health monitoring", *Proceedings of the 2nd Infrastructure Theme Postgraduate Conference*: *Rethinking Sustainable Development-Planning*, *Infrastructure Engineering*, *Design and Managing Urban Infrastructure*, Brisbane, Australia, pp. 35-47.
Wang, Z., Yan, W. and Oates, T. (2017), "Time series classification from scratch with deep neural networks: A strong baseline", *Proceedings of 2017 International Joint Conference on Neural Networks* (*IJCNN*), Anchorage, AK, USA, May, pp. 1578-1585. https://doi.org/10.1109/IJCNN.2017.7966039
Xing, Z., Pei, J. and Keogh, E. (2010), "A brief survey on sequence classification", *ACM Sigkdd Explorations Newsletter*,

12(1), 40-48. https://doi.org/10.1145/1882471.1882478
Xu, N. and Liu, Y. (2021), "Fractal-based manifold learning for structure health monitoring", In: *AIAA Scitech 2021 Forum*, p. 1167. https://doi.org/10.2514/6.2021-1167
Xu, H., Gao, Y., Yu, F. and Darrell, T. (2017), "End-to-end learning of driving models from large-scale video datasets", *Proceedings of the IEEE Conference on Computer Vision and Pattern Recognition*, pp. 2174-2182.
Xu, Y., Bao, Y., Chen, J., Zuo, W. and Li, H. (2019), "Surface fatigue crack identification in steel box girder of bridges by a deep fusion convolutional neural network based on consumer-grade camera images", *Struct. Health Monitor.*, **18**(3), 653-674. https://doi.org/10.1177/1475921718764873
Yang, Y., Li, S., Nagarajaiah, S., Li, H. and Zhou, P. (2016), "Real-time output-only identification of time-varying cable tension from accelerations via complexity pursuit", *J. Struct. Eng.*, **142**(1), 04015083. https://doi.org/10.1061/(ASCE)ST.1943-541X.0001337
Ye, X.W., Dong, C.Z. and Liu, T. (2016), "Force monitoring of steel cables using vision-based sensing technology: methodology and experimental verification", *Smart Struct. Syst., Int. J.*, **18**(3), 585-599. https://doi.org/10.12989/sss.2016.18.3.585
Zhang, Z. (2020), "Data-Driven and Model-Based Methods with Physics-Guided Machine Learning for Damage Identification", Ph.D. Thesis; Louisiana State University.
Zhang, Z. and Sun, C. (2020a), "Multi-site structural damage identification using a multi-label classification scheme of machine learning", *Measurement*, **154**, 107473. https://doi.org/10.1016/j.measurement.2020.107473
Zhang, Z. and Sun, C. (2020b), "Structural damage identification via physics-guided machine learning: a methodology integrating pattern recognition with finite element model updating", *Struct. Health Monitor.*, **20**(4), 1675-1688. https://doi.org/10.1177/1475921720927488
Zhang, Z. and Sun, C. (2020c), "A numerical study on multi-site damage identification: A data-driven method via constrained independent component analysis", *Struct. Control Health Monitor.*, **27**(10), e2583. https://doi.org/10.1002/stc.2583
Zhang, Z., Sun, C., Li, C. and Sun, M. (2019a), "Vibration based bridge scour evaluation: A data-driven method using support vector machines", *Struct. Monitor. Maint., Int. J.*, **6**(2), 125-145. https://doi.org/10.12989/smm.2019.6.2.125
Zhang, W., Jin, F., Zhang, G., Zhao, B. and Hou, Y. (2019b), "Aero-engine remaining useful life estimation based on 1-dimensional FCN-LSTM neural networks", *Proceedings of 2019 Chinese Control Conference* (*CCC*), Guangzhou, China, July, pp. 4913-4918. https://doi.org/10.23919/ChiCC.2019.8866118
Zhang, R., Liu, Y. and Sun, H. (2020), "Physics-informed multi-LSTM networks for metamodeling of nonlinear structures", *Comput. Methods Appl. Mech. Eng.*, **369**, 113226. https://doi.org/10.1016/j.cma.2020.113226
Zhang, Z., Sun, C. and Guo, B. (2021), "Transfer-learning guided Bayesian model updating for damage identification considering modeling uncertainty", *Mech. Syst. Signal Process.*, **166**, 108426. https://doi.org/10.1016/j.ymssp.2021.108426
Zheng, Y., Liu, Q., Chen, E., Ge, Y. and Zhao, J.L. (2014), "Time series classification using multi-channels deep convolutional neural networks", *Proceedings of International Conference on Web-Age Information Management*, pp. 298-310. https://doi.org/10.1007/978-3-319-08010-9_33
Zheng, S., Ristovski, K., Farahat, A. and Gupta, C. (2017), "Long short-term memory network for remaining useful life estimation", *Proceedings of 2017 IEEE International Conference on Prognostics and Health Management* (*ICPHM*), Dallas, TX, USA, June, pp. 88-95.